JACS
JOURNAL OF THE AMERICAN CHEMICAL SOCIETY
Communication
pubs.acs.org/JACS

Discrete Bimodal Probes for Thrombus Imaging

Ritika Uppal,[†] Kate L. Ciesienski, Daniel B. Chonde, Galen S. Loving, and Peter Caravan*

A. A. Martinos Center for Biomedical Imaging, Massachusetts General Hospital, Harvard Medical School, 149 13th Street, Suite 2301, Charlestown, Massachusetts 02129, United States

Supporting Information

ABSTRACT: Here we report a generalizable solid/solution-phase strategy for the synthesis of discrete bimodal fibrin-targeted imaging probes. A fibrin-specific peptide was conjugated with two distinct imaging reporters at the C- and N-termini. In vitro studies demonstrated retention of fibrin affinity and specificity. Imaging studies showed that these probes could detect fibrin over a wide range of probe concentrations by optical, magnetic resonance, and positron emission tomography imaging.

Thrombosis, the formation of a blood clot within an artery or vein, is implicated in many of the leading causes of death worldwide: heart attack, stroke, pulmonary embolism, and deep vein thrombosis.[1] The in vivo detection and characterization of thrombus is essential for diagnosing disease, guiding therapy, and monitoring treatment. Several imaging modalities can be used for noninvasive identification of thrombus in a clinical or preclinical setting, and these include positron emission tomography (PET), magnetic resonance imaging (MRI), and optical imaging (OI). Each modality has its own strengths and weaknesses; therefore, combinations of modalities are increasingly used to provide synergies.[2−5] Concurrently, multimodal imaging probes are being developed to exploit the gains in hybrid imaging systems for the improved detection of disease.[6−9] We present here thrombus-targeted imaging probes employing positron emitters, MRI relaxation agents, and fluorophores.

For molecular imaging of thrombus-related biomarkers, fibrin offers the potential for high disease specificity and sensitivity. This is because fibrin is present in all thrombi but is found only in clots and not in circulating blood. Discrete peptide-based probes,[10−17] antibodies,[18] and nanoparticles[19−24] have been used to image fibrin. For imaging of solid thrombi, peptide-based probes may be more advantageous than antibodies or nanoparticles because their small size offers higher potential to penetrate the clot. However, unlike nanoparticles, which are insensitive to the incorporation of multiple imaging reporters, it is a challenge to modify a short peptide with two imaging reporters and still maintain target affinity and specificity.[9] For instance, the incorporation of hydrophobic fluorescent dyes may induce nonspecific protein binding.[25] We reasoned that conjugation of a hydrophilic metal complex might offset the hydrophobicity introduced by the organic dye. To minimize the impact of the imaging reporters on fibrin binding, we positioned one reporter at the N-terminus and the other at the C-terminus of the peptide. To this end, we describe fluorescent/MRI- and fluorescent/PET-labeled peptides that maintain fibrin affinity and specificity after derivatization.

In our previous work, we noted that derivatizing both the C- and N-termini of fibrin-specific peptides with Gd chelates not only increased the detection sensitivity but also protected those probes from exopeptidase degradation.[26] Peptide substitutions at the C- and N-termini were relatively insensitive to fibrin affinity, presumably because of the conformational rigidity imparted by the cyclic peptide core. To introduce different imaging reporters, we reasoned that a mixed solid/solution-phase synthetic approach could be used to incorporate a fluorophore (OI) at one terminus and a chelator for Gd (MRI) or ^{64}Cu (PET) at the other terminus. The probe synthesis is outlined in Scheme 1. The peptide and N-terminal modification are synthesized on resin. After resin cleavage, deprotection, and cyclization, the C-terminus is modified in solution. Complexation with Gd^{3+} or $^{64}Cu^{2+}$ is the final synthetic step.

Scheme 1. Mixed Solid/Solution-Phase Synthesis of Multimodal Probes (See the SI for Full Synthetic Details)

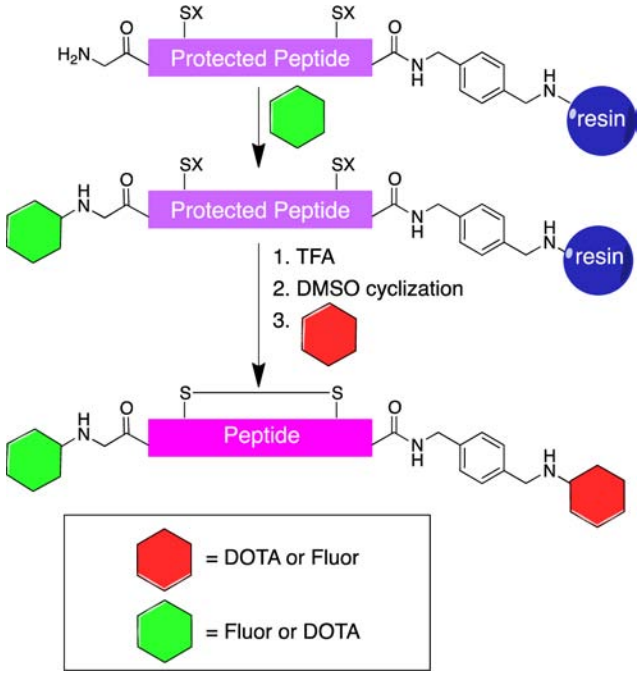

In our probe design, we employed the established fibrin-specific cyclic peptide used in the MRI thrombus agent EP-2104R and maintained the modification with *p*-xylenediamine to

Received: May 10, 2012
Published: June 14, 2012

dx.doi.org/10.1021/ja3045635 | J. Am. Chem. Soc. 2012, 134, 10799−10802

introduce a primary amine at the C-terminus.[14] Fluorescein isothiocyanate (FITC) was used to incorporate a fluorescent reporter at the C-terminus. For attachment of FITC at the N-terminus, it was necessary to introduce a linker, since direct thiourea bond formation at the N-terminus is not stable under the peptide deprotection conditions. The tris(*tert*-butyl) ester of 1,4,7,10-tetraazacyclododecane-1,4,7,10-tetraacetic acid (DOTA) was used to couple the chelate as a monoamide to either the C- or N-terminus. After removal of the *tert*-butyl protecting groups, either Gd(III) or Cu(II) was introduced. The probes are denoted Fl-^{N}Pep-Gd, etc., where Fl is fluorescein, Gd is GdDOTA monoamide, Cu is CuDOTA monoamide, and ^{N}Pep refers to the peptide; in the example Fl-^{N}Pep-Gd, the fluorescein is conjugated to the N-terminus. Full synthetic details are described in the Supporting Information (SI).

Binding of the probes to human fibrin was assessed in a plate-based assay as previously described.[10,14] In this assay, aliquots of fibrinogen solution are dispensed into a 96-well plate and then polymerized to fibrin by addition of $CaCl_2$ and thrombin. The fibrin gel is then dried onto the base of the plate by evaporation at 37 °C. Rehydration with an equivalent volume of liquid results in a known concentration of polymeric fibrin based on fibrinogen monomer. Solutions of Gd-^{N}Pep-Fl, Cu-^{N}Pep-Fl, and Fl-^{N}Pep-Gd ranging from 0.1 to 50 μM in either Tris-buffered saline (TBS) or citrated rat plasma were added to each of the wells of a dried fibrin (7 μM) microtiter plate. After 2 h of incubation, the concentration of free probe, [free], was assayed by ICP-MS or fluorescence-HPLC. The concentration of fibrin-bound species, [bound], in the clot was determined by subtraction as [bound] = [total] − [free]. The binding data were fit to a stoichiometric binding model with stepwise association constants K_1, K_2 and K_3 (Figure S1 in the SI). The affinities of Gd-^{N}Pep-Fl and Fl-^{N}Pep-Gd for human fibrin (Table 1) were similar and comparable to that of EP-2104R. Not surprisingly, replacement of Gd(III) with Cu(II) did not significantly change the fibrin affinity of the probe.

Table 1. Stepwise Association Constants for Binding of Bimodal Probes to Human Fibrin Measured in Buffer (B) or Blood Plasma (P)[a]

compound	K_1	K_2	K_3
Fl-^{N}Pep-Gd (B)	0.89 (0.25)	0.23 (0.09)	0.018 (0.006)
Gd-^{N}Pep-Fl (B)	1.00 (0.34)	0.19 (0.11)	0.23 (0.11)
Gd-^{N}Pep-Fl (P)	0.53 (0.08)	0.064 (0.029)	0.05 (0.034)
Cu-^{N}Pep-Fl (B)	0.75 (0.29)	0.34 (0.18)	0.14 (0.06)
EP-2104R	1.01 (0.39)	0.18 (0.06)	NA[b]

[a] K_i values are given in μM^{-1}. Standard deviations are given in parentheses. [b] NA= not applicable.

One concern with using organic fluorophores for in vivo applications is the potential for nonspecific binding of the hydrophobic fluorophore. Nonspecific protein binding would adversely impact the distribution of the probe and its specificity for fibrin in vivo. In our previous work with this type of peptide, we found that peptide derivatives bind to two equivalent binding sites on fibrin.[10,14] When fluorescein is incorporated into the molecule, there is a third, weaker fibrin binding event that we attribute to a nonspecific interaction. We were concerned that nonspecific binding to other proteins could lower the effective affinity of the probe for fibrin, so we measured fibrin affinity in the presence of blood plasma proteins. However, the apparent fibrin affinity of Gd-^{N}Pep-Fl measured in rat plasma was only 2–3-fold lower than that measured in buffer (Table 1), indicating that this probe maintains high specificity for fibrin.

The relaxivities of the Gd-containing probes as well as the commercial contrast agent [Gd(HP-DO3A)(H_2O)] (ProHance, gadoteridol) were measured at 1.4 T and 37 °C in either pH 7.4 TBS, 30 μM fibrinogen (fgn) solution in TBS, or 30 μM fibrin gel in TBS (Table 2). The relaxivities in TBS are much higher than for small Gd(III) complexes such as [Gd(HP-DO3A)(H_2O)], and this relaxivity increase is due to the increased molecular weight, which results in slower rotational diffusion. Protein binding further decreases the correlation time and results in increased relaxivity.[27] This is reflected by the 50% higher relaxivity of Fl-^{N}Pep-Gd in fibrin gel than in buffer alone. On the other hand, little to no increase in relaxivity was observed in fgn solution, implying that these probes do not bind fibrinogen as was seen previously with this peptide sequence. The lack of fibrinogen binding is important since there is ~7 μM fibrinogen in circulating blood plasma. The specificity of the probes for fibrin over the structurally similar fibrinogen precursor may be expected to enhance the target:background ratio in vivo. In addition, there was no change in the relaxivity of [Gd(HP-DO3A)(H_2O)] when measured in TBS, fgn, or fibrin gel, suggesting no protein binding and indicating that the mechanical properties of the gel do not affect the relaxivity. We note that the relaxivities of the probes in the presence of fibrin (21.2 mM^{-1} s^{-1} for Gd-^{N}Pep-Fl and 18.8 mM^{-1} s^{-1} for Fl-^{N}Pep-Gd) are quite high at this clinically relevant field strength and comparable to those of other high-relaxivity compounds such as fibrin-bound EP-2104R and albumin-bound MS-325 at 1.4 T.[14,28] The relaxivity will decrease with increasing field strength, but on the basis of the field dependence of the relaxivities of related molecules,[29] we expect higher relaxivities than for simple Gd(III) chelates at fields up to 9.4 T.

Table 2. Relaxivities of Gd-Containing Probes Measured at 1.4 T and 37 °C in pH 7.4 TBS, 30 μM Fibrinogen (fgn) Solution in TBS, or 30 μM Fibrin Gel in TBS[a]

compound	TBS	fgn	fibrin
Fl-^{N}Pep-Gd	12.5	11.4	18.8
Gd-^{N}Pep-Fl	16.4	17.6	21.2
[Gd(HP-DO3A)(H_2O)]	3.00	3.04	3.04

[a] Relaxivities are given in mM^{-1} s^{-1}. Uncertainties are estimated to be ±10%.

The relaxivity results were corroborated by imaging studies on a clinical 1.5 T MRI scanner. Here we compared the commercial contrast agent [Gd(HP-DO3A)(H_2O)] with equimolar Gd-^{N}Pep-Fl. Figure 1 shows T_1-weighted MRI images of six tubes containing water, fgn solution, or fgn solution polymerized to fibrin gel and then separated by mechanical agitation. Tubes A and B contained no Gd and represent the baseline signal intensity. Tubes C and D contained 25 μM [Gd(HP-DO3A)-(H_2O)] in fgn and fibrin gel, respectively. There was a slight enhancement in signal (16.5%) relative to tube B due to the dilute low-relaxivity contrast agent. However, the enhancement was uniform in both C and D, indicating that [Gd(HP-DO3A)(H_2O)] could not distinguish the fibrin clot on the wall of tube D from the unclotted solution. Tube E contained equimolar Gd-^{N}Pep-Fl in fgn solution, and the signal enhancement (59% relative to tube B) was much greater than for [Gd(HP-DO3A)(H_2O)] as a result of the higher relaxivity of Gd-^{N}Pep-Fl. Tube F shows that when a fibrin clot was prepared

dx.doi.org/10.1021/ja3045635 | J. Am. Chem. Soc. 2012, 134, 10799–10802

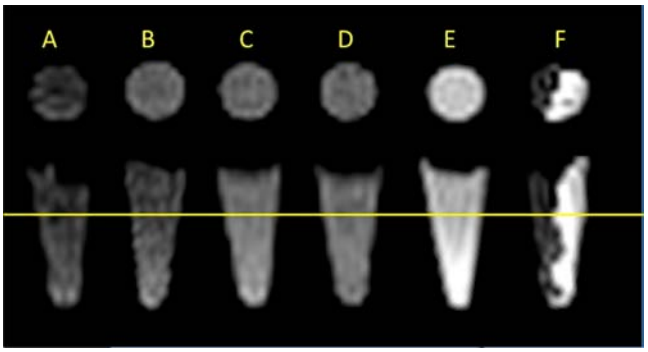

Figure 1. MRI of fibrinogen (fgn) solutions and fibrin clots. Six 1 mL centrifuge tubes were scanned on a clinical 1.5 T MRI at room temperature. The top row shows axial slices corresponding to the plane indicated by the line through the coronal images shown in the bottom row. (A) pure water; (B) 15 μM fgn; (C) 25 μM [Gd(HP-DO3A)] in 15 μM fgn; (D) 25 μM [Gd(HP-DO3A)] in 15 μM fibrin gel; (E) 25 μM Gd-^{N}Pep-Fl in 15 μM fgn; (F) 25 μM Gd-^{N}Pep-Fl in 15 μM fibrin gel.

and separated, Gd-^{N}Pep-Fl localized in the clot and generated high clot signal intensity (156% increase relative to tube B) and strong contrast between the clot and the supernatant with a very high contrast-to-noise ratio of 39.

We performed a similar experiment using a IVIS fluorescence spectrum imager. Figure 2 compares 50 nM Gd-^{N}Pep-Fl to

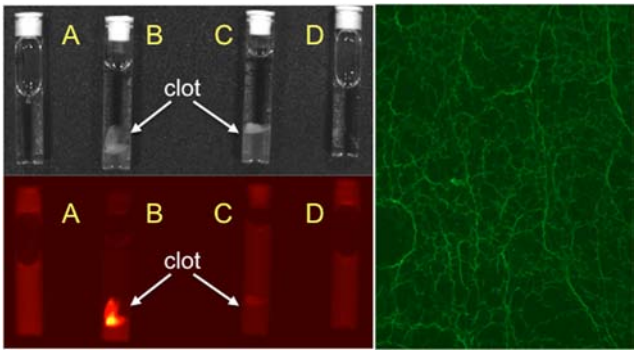

Figure 2. Fluorescence images of fibrinogen (fgn) and fibrin clots. Phantoms (A–D) were scanned on an IVIS spectrum imager (left panels). Fluorescence images (bottom left) are overlaid on photographs (top left) of 1 mL glass tubes containing 1 mL of (A) 50 nM Gd-^{N}Pep-Fl in 6 μM fgn; (B) 50 nM Gd-^{N}Pep-Fl in 6 μM fibrin gel; (C) 50 nM fluorescein in 6 μM fibrin gel; or (D) 50 nM fluorescein in 6 μM fgn. Right panel: fluorescence confocal microscopy image of fibrinogen polymerized on a microscopy slide in the presence of Gd-^{N}Pep-Fl.

equimolar fluorescein in either fgn solution or a separated fibrin clot. In this study, fgn was clotted (tubes B and C), and the tubes were centrifuged to separate the clot from the supernatant, as is apparent from the photograph of the tubes (Figure 2, top left). The fluorescence image overlaid on the photograph clearly shows that Gd-^{N}Pep-Fl was localized in the clot and depleted from the supernatant, whereas untargeted fluorescein was evenly distributed between the clot and the supernatant. The right panel in Figure 2 shows a fluorescence confocal microscopy image of a fibrin gel in the presence of Gd-^{N}Pep-Fl. The probe highlights the weblike fibrin mesh at the microscopic level.

Finally, we compared the ^{64}Cu versions of both probes to ^{64}CuDOTA in a similar experimental paradigm using PET imaging on a clinical PET scanner. The images in Figure 3 demonstrate that the dual probes can visualize fibrin with PET

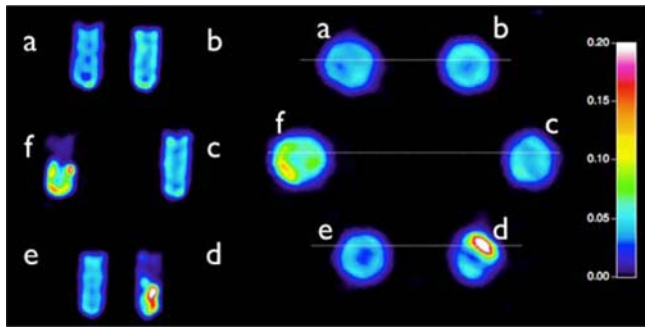

Figure 3. PET imaging of fibrinogen solutions (fgn) and fibrin clots. Phantoms in 4 mL glass culture tubes were scanned on a clinical PET head scanner. Each phantom contained fibrinogen (fgn) at a final concentration of 6 μM, 2.3 nmol of peptide or DOTA, a total volume of 2 mL, and a total activity of 10 μCi. (A) ^{64}CuDOTA in fgn; (B) ^{64}CuDOTA in fibrin gel; (C) Fl-^{N}Pep-^{64}Cu in fgn; (D) Fl-^{N}Pep-^{64}Cu in fibrin gel; (E) ^{64}Cu-^{N}Pep-Fl in fgn; (F) ^{64}Cu-^{N}Pep-Fl in fibrin gel.

imaging. In the fgn solutions (Figure 3A,C,E), the ^{64}Cu was distributed equally throughout the samples, giving rise to uniform signal intensity. When the fgn was clotted and the tube spun down (tube B), there was no difference in the PET image between tubes A and B, indicating that untargeted ^{64}CuDOTA cannot be used to detect fibrin. The ^{64}CuDOTA was distributed equally in the clot (at the bottom of tube B) and in the liquid above the clot. The ^{64}CuDOTA experiment also demonstrates that clot formation does not physically trap the molecule. On the other hand, the fibrin-targeted dual probes both demonstrated an ability to detect fibrin. Tubes D and F indicate that the radioactivity was centered in the bottom of each tube (i.e., in the clot) with very little activity remaining in the liquid above the clot.

In conclusion, we have described four new fibrin-targeting probes that can be modified to be detectable in multiple modalities and still maintain fibrin affinity and specificity. These bimodal probes offer the opportunity to image fibrin over a range of spatial resolutions (OI > MRI > PET) and detection sensitivities (PET > OI > MRI). This proof-of-concept study utilized inexpensive reagents, but our mixed solid/solution-phase synthesis is generalizable and amenable to incorporating any bifunctional chelator or fluorophore using standard amine bioconjugation techniques. Combinations of labels may have important applications where high-sensitivity, low-resolution PET imaging can detect the presence of thrombus throughout the body and then be used to guide where high-resolution MRI or catheter-based OI should be performed. For instance, one such clinical application could be to detect the presence of coronary artery thrombus and guide stent placement.

■ ASSOCIATED CONTENT

Ⓢ Supporting Information

Experimental procedures; probe synthesis and characterization; and details of fibrin binding, relaxivity, and imaging measurements. This material is available free of charge via the Internet at http://pubs.acs.org.

■ AUTHOR INFORMATION

Corresponding Author

caravan@nmr.mgh.harvard.edu

Present Address

[†]GE Healthcare, Medical Diagnostics, Bangalore, India.

Notes

The authors declare the following competing financial interest(s): P.C. has equity in Factor 1A, LLC, the company that holds the patent rights to the peptides used in these probes.

■ ACKNOWLEDGMENTS

Thomas Benner and Zdravka Medarova are thanked for assistance in the MRI and OI studies. This work was supported in part by Awards R01HL109448, R01EB009062, T32CA009502, and P41RR14075 from the National Institutes of Health.

■ REFERENCES

(1) Roger, V. L.; Go, A. S.; Lloyd-Jones, D. M.; Benjamin, E. J.; Berry, J. D.; Borden, W. B.; Bravata, D. M.; Dai, S.; Ford, E. S.; Fox, C. S.; Fullerton, H. J.; Gillespie, C.; Hailpern, S. M.; Heit, J. A.; Howard, V. J.; Kissela, B. M.; Kittner, S. J.; Lackland, D. T.; Lichtman, J. H.; Lisabeth, L. D.; Makuc, D. M.; Marcus, G. M.; Marelli, A.; Matchar, D. B.; Moy, C. S.; Mozaffarian, D.; Mussolino, M. E.; Nichol, G.; Paynter, N. P.; Soliman, E. Z.; Sorlie, P. D.; Sotoodehnia, N.; Turan, T. N.; Virani, S. S.; Wong, N. D.; Woo, D.; Turner, M. B. *Circulation* **2012**, *125*, 188.

(2) Beyer, T.; Freudenberg, L. S.; Czernin, J.; Townsend, D. W. *Insights Imaging* **2011**, *2*, 235.

(3) Catana, C.; Procissi, D.; Wu, Y.; Judenhofer, M. S.; Qi, J.; Pichler, B. J.; Jacobs, R. E.; Cherry, S. R. *Proc. Natl. Acad. Sci. U.S.A.* **2008**, *105*, 3705.

(4) Schlemmer, H. P.; Pichler, B. J.; Schmand, M.; Burbar, Z.; Michel, C.; Ladebeck, R.; Jattke, K.; Townsend, D.; Nahmias, C.; Jacob, P. K.; Heiss, W. D.; Claussen, C. D. *Radiology* **2008**, *248*, 1028.

(5) Townsend, D. W. *J. Nucl. Med.* **2008**, *49*, 938.

(6) Frullano, L.; Catana, C.; Benner, T.; Sherry, A. D.; Caravan, P. *Angew. Chem., Int. Ed.* **2010**, *49*, 2382.

(7) Frullano, L.; Meade, T. J. *J. Biol. Inorg. Chem.* **2007**, *12*, 939.

(8) Jaffer, F. A.; Libby, P.; Weissleder, R. *Arterioscler., Thromb., Vasc. Biol.* **2009**, *29*, 1017.

(9) Kuil, J.; Velders, A. H.; van Leeuwen, F. W. *Bioconjugate Chem.* **2010**, *21*, 1709.

(10) Kolodziej, A. F.; Nair, S. A.; Graham, P.; McMurry, T. J.; Ladner, R. C.; Wescott, C.; Sexton, D. J.; Caravan, P. *Bioconjugate Chem.* **2012**, *23*, 548.

(11) Makowski, M. R.; Forbes, S. C.; Blume, U.; Warley, A.; Jansen, C. H.; Schuster, A.; Wiethoff, A. J.; Botnar, R. M. *Atherosclerosis* **2012**, *222*, 43.

(12) Miserus, R. J.; Herias, M. V.; Prinzen, L.; Lobbes, M. B.; Van Suylen, R. J.; Dirksen, A.; Hackeng, T. M.; Heemskerk, J. W.; van Engelshoven, J. M.; Daemen, M. J.; van Zandvoort, M. A.; Heeneman, S.; Kooi, M. E. *JACC Cardiovasc. Imaging* **2009**, *2*, 987.

(13) Nair, S. A.; Kolodziej, A. F.; Bhole, G.; Greenfield, M. T.; McMurry, T. J.; Caravan, P. *Angew. Chem., Int. Ed.* **2008**, *47*, 4918.

(14) Overoye-Chan, K.; Koerner, S.; Looby, R. J.; Kolodziej, A. F.; Zech, S. G.; Deng, Q.; Chasse, J. M.; McMurry, T. J.; Caravan, P. *J. Am. Chem. Soc.* **2008**, *130*, 6025.

(15) Uppal, R.; Ay, I.; Dai, G.; Kim, Y. R.; Sorensen, A. G.; Caravan, P. *Stroke* **2010**, *41*, 1271.

(16) Uppal, R.; Catana, C.; Ay, I.; Benner, T.; Sorensen, A. G.; Caravan, P. *Radiology* **2011**, *258*, 812.

(17) Zhang, Z.; Kolodziej, A. F.; Greenfield, M. T.; Caravan, P. *Angew. Chem., Int. Ed.* **2011**, *50*, 2621.

(18) Morris, T. A.; Gerometta, M.; Yusen, R. D.; White, R. H.; Douketis, J. D.; Kaatz, S.; Smart, R. C.; Macfarlane, D.; Ginsberg, J. S. *Am. J. Respir. Crit. Care Med.* **2011**, *184*, 708.

(19) Cai, K.; Kiefer, G. E.; Caruthers, S. D.; Wickline, S. A.; Lanza, G. M.; Winter, P. M. *NMR Biomed.* **2012**, *25*, 279.

(20) McCarthy, J. R.; Patel, P.; Botnaru, I.; Haghayeghi, P.; Weissleder, R.; Jaffer, F. A. *Bioconjugate Chem.* **2009**, *20*, 1251.

(21) Pan, D.; Caruthers, S. D.; Hu, G.; Senpan, A.; Scott, M. J.; Gaffney, P. J.; Wickline, S. A.; Lanza, G. M. *J. Am. Chem. Soc.* **2008**, *130*, 9186.

(22) Pan, D.; Caruthers, S. D.; Senpan, A.; Yalaz, C.; Stacy, A. J.; Hu, G.; Marsh, J. N.; Gaffney, P. J.; Wickline, S. A.; Lanza, G. M. *J. Am. Chem. Soc.* **2011**, *133*, 9168.

(23) Pan, D.; Pramanik, M.; Senpan, A.; Yang, X.; Song, K. H.; Scott, M. J.; Zhang, H.; Gaffney, P. J.; Wickline, S. A.; Wang, L. V.; Lanza, G. M. *Angew. Chem., Int. Ed.* **2009**, *48*, 4170.

(24) Pan, D.; Roessl, E.; Schlomka, J. P.; Caruthers, S. D.; Senpan, A.; Scott, M. J.; Allen, J. S.; Zhang, H.; Hu, G.; Gaffney, P. J.; Choi, E. T.; Rasche, V.; Wickline, S. A.; Proksa, R.; Lanza, G. M. *Angew. Chem., Int. Ed.* **2010**, *49*, 9635.

(25) Choi, H. S.; Nasr, K.; Alyabyev, S.; Feith, D.; Lee, J. H.; Kim, S. H.; Ashitate, Y.; Hyun, H.; Patonay, G.; Strekowski, L.; Henary, M.; Frangioni, J. V. *Angew. Chem., Int. Ed.* **2011**, *50*, 6258.

(26) Zhang, Z.; Kolodziej, A. F.; Qi, J.; Nair, S. A.; Wang, X.; Case, A. W.; Greenfield, M. T.; Graham, P. B.; McMurry, T. J.; Caravan, P. *New J. Chem.* **2010**, *2010*, 611.

(27) Caravan, P.; Ellison, J. J.; McMurry, T. J.; Lauffer, R. B. *Chem. Rev.* **1999**, *99*, 2293.

(28) Caravan, P.; Cloutier, N. J.; Greenfield, M. T.; McDermid, S. A.; Dunham, S. U.; Bulte, J. W.; Amedio, J. C., Jr.; Looby, R. J.; Supkowski, R. M.; Horrocks, W. D., Jr.; McMurry, T. J.; Lauffer, R. B. *J. Am. Chem. Soc.* **2002**, *124*, 3152.

(29) Caravan, P.; Farrar, C. T.; Frullano, L.; Uppal, R. *Contrast Media Mol. Imaging* **2009**, *4*, 89.